PCCP

Accepted Manuscript

ROYAL SOCIETY OF CHEMISTRY

www.rsc.org/pccp

Journal Name

ARTICLE TYPE

Cite this: DOI: 10.1039/xxxxxxxxxx

Theoretical Study of the Dark Photochemistry of 1,3-Butadiene via the Chemiexcitation of Dewar Dioxetane

Pooria Farahani,*[a,b] Marcus Lundberg,[a] Roland Lindh,[a] and Daniel Roca-Sanjuán*[b]

Received Date
Accepted Date

DOI: 10.1039/xxxxxxxxxx

www.rsc.org/journalname

Excited-state chemistry is usually ascribed to photo-induced processes, such as fluorescence, phosphorescence, and photochemistry, or to bio- and chemiluminescence, in which light emission is originated by a chemical reaction. A third class of excited-state chemistry is, however, possible. It corresponds to the photochemical phenomena produced by chemienergizing certain chemical groups without light - chemiexcitation. By studying Dewar dioxetane, which can be viewed as the combination of 1,2-dioxetane and 1,3-butadiene, we show here how the photo-isomerization channel of 1,3-butadiene can be reached at a later stage after the thermal decomposition of the dioxetane moiety. Multi-reference multiconfigurational quantum chemistry methods and accurate reaction-path computational strategies were used to determine the reaction coordinate of three succesive processes: decomposition of the dioxetane moiety, non-adiabatic energy transfer from the the ground to the excited state, and finally non-radiative decay of the 1,3-butadiene group. With the present study, we open a new area of research within computational photochemistry to study chemically-induced excited-state chemistry that is difficult to tackle experimentally due to the short-lived character of the species involved in the process. The findings shall be of relevance to unveil "dark" photochemistry mechanisms which might operate in biological systems in conditions of lack of light. These mechanisms might allow reactions that are typical of photo-induced phenomena.

1 Introduction

Photochemistry usually implies the production of new chemical species by photo exciting the initial compound. In this process, the molecule is promoted from the ground to the excited electronic state by means of irradiation with light, enabling reactivity that is not present in the thermochemistry of the compound. Nevertheless, radiation is not the only source for electronic excitation. Excited states can be also generated by chemically energizing a molecule, as evidenced by the phenomenon of chemiluminescence and bioluminescence. Therefore, it is natural to expect that the reactions that are typical of photo-induced processes might be also produced without light by using a chemiluminophore, i.e., a species with special properties for an efficient population transfer from a ground to a excited state.[1] This unconventional manner of photochemistry has been called in the literature *dark photochemistry*, which is the name that we will use here to be consistent with previous studies. In the context of dark photochemistry, two possibilities arise for chemienergizing a molecule M (see Fig. 1), either by (a) intra-molecular energy transfer from a chemiluminophore (CL) or sensitizer that has been attached to the target molecule (M) or by (b) inter-molecular energy transfer between isolated CL to M compounds These versions were termed by Zimmerman and Keck as *vertical* and *non-vertical* dark photochemistry, respectively.[2] Clearly, the non-vertical process might introduce complexity in the synthesis of an appropriate reactant. However, it has the advantage that the excited state is generated directly by a skeletal rearrangement of the structure, without involving less-efficient inter-molecular processes. In contrast to the photo-induced phenomena, both chemical sensitizations (a) and (b) allow their use in cases where light is absent. This might be relevant for biorganisms living in caves or in the deep sea and it has interesting applications in technology. For example, Ermoshkin *et al.*[3] showed how to produce "photopolymers" inside dark tubes or behind a pipe.

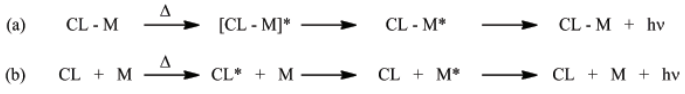

Fig. 1 Intra-molecular (i) and inter-molecular (ii) chemical production of excited states.

Dark photochemisty was initially studied in the 70s and 80s

[a] *Department of Chemistry –Ångström, Uppsala University, P.O. Box 518, SE-751 20 Uppsala, Sweden; E-mail: farahani.pooria@gmail.com, Daniel.Roca@uv.es*
[b] *Instituto de Ciencia Molecular, Universitat de València, P.O. Box 22085, ES-46071 València, Spain.*
* To whom correspondence should be addressed.

† Electronic Supplementary Information (ESI) available: [Cartesian coordinates; electronic, zero-point vibrational, and Gibbs free energies; spin-orbit coupling values; CASPT2//CASSCF minimum energy path for the ground-state dissociation after the C_2-C'_2 bond cleavage]. See DOI: 10.1039/b000000x/

mainly by Cilento, Adam, and co-workers,[4,5] among others.[2,6–8] Since then, transformations of excited triplet and singlet species chemically produced in the thermolysis of dioxetanes, dioxetanones, or oxalates have been used for the determination of chemiexcitation yields.[4,5,9] In addition, the chemienergetic species have been used to induce excited-state chemistry of target molecules by energy transfer.[9–11] Similar phenomena have been postulated to occur in biological systems catalyzed by enzymes such as peroxidases since the excited species were of the type expected from cleavage of a dioxetane/dioxetanone intermediate.[4,5,12] Some illustrative examples are the detection of thymine dimers in the calf thymus DNA treated with trimethyl-1,2-dioxetane without UV radiation[13,14], the oxidative DNA damage by radicals generated via the chemiexcitation of ketones,[15] the production of the plant hormone ethylene from enzymatically generated triplet 1-butanal,[16] or the opening of the B-ring of protovitamins D through triplet sensitization in the isobutyraldehyde/peroxidase/O_2 system.[5] As described by White *et al.*,[17] the model system in the second example might be relevant for understanding how vitamin D is formed in certain species in complete darkness. A more recent example is the study performed by Mano *et al.*[18] who have demonstrated the enzymatic generation of singlet molecular oxygen from excited triplet carbonyls.

In contrast to the dark photochemistry originated by energy transfer (Fig. 1b), intra-molecular sensitization (Fig. 1a) has been much less exploited.[4,5] Recently, Motoyoshiya *et al.*[9] have carried out a study comparing the efficiency of the *cis-trans* isomerization of stilbene induced by energy transfer from a peroxylate with that of the process promoted by intra-sensitization from a molecular system in which stilbene is covalently linked to the peroxylate. Higher efficiency is reported for the later. However, the conclusion might not be straightforward because many authors indicate that the actual chemiluminophore in the chemiluminescence of peroxylate systems is the dioxetanedione molecule and not the original peroxylate.[19] Hence, if this is the case, the intra-molecular sensitization of stilbene would not happen.

To explain the ability of the chemiluminophores to generate electronic excited states and produce dark photochemistry, a throughout understanding of the mechanism is essential. This is a difficult task from an experimental standpoint because dioxetanes are labile systems. In fact, the thermal dissociation mechanism of the simple 1,2-dioxetane molecule has still not been experimentally demonstrated. Two extreme views have been proposed: the concerted mechanism, in which the O-O' and C-C' bond cleavages occur simultaneously, and the biradical mechanism, in which a biradical intermediate is formed in between the rupture of the O-O' and C-C' bonds.[20] Trapping experiments cannot solve the problem due to the seemingly short lifetimes of the biradicals. In this context, *ab initio* quantum chemistry arises as a relevant tool to shed light on the dissociation mechanism of dioxetanes and related systems. Recently, the mechanism of 1,2-dioxetane has been established by these means to be of biradical type.[21] Moreover, accurate theoretical approaches have been employed successfully to determine the chemiluminescence mechanism of dioxetanone,[22–24] small models of the Firefly luciferin and coelenterazine,[25,26] and the Firefly luciferin[27,28] and coelenterazine[29,30] systems themselves. Quantum chemistry may, therefore, be applied to study how photochemical processes can be induced chemically "in darkness". One appropriate molecular system for such purpose, taking into account its relatively small size, is Dewar dioxetane, which combines 1,2-dioxetane and 1,3-butadiene in the same molecule (see Fig. 2). This compound facilitates the study of the dark photochemistry in the shortest polyene, 1,3-butadiene.

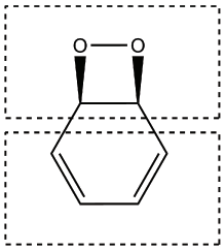

Fig. 2 Dewar dioxetane is composed by 1,3-butadiene (bottom) and 1,2-dioxetane (top).

Dewar dioxetane has been already discussed in the literature in a couple of experimental works.[12,31] McCapra referred to it in the study of the isomerization of Dewar benzene into benzene in the excited state (see Fig. 3a).[31] According to the Woodward-Hoffmann rule, this transformation is symmetry-forbidden.[32] Indeed, the activation energy of 90 kcal/mol, reported by McCapra, prevents the benzene product to be achieved thermally (see Fig. 3a). However, light emission was observed in the thermal decomposition. In addition, the luminescence showed a dependence on the presence of oxygen. Therefore, on the basis of these observations, McCapra proposed the reaction in Fig. 3b as a possible mechanism to explain the observed light. It implies the oxidation of Dewar benzene, which generates a species with the 1,2-dioxetane chemical functionality, the Dewar dioxetane molecule.

Dewar dioxetane has also been proposed as a relevant structure in the enzymatic oxidation of benzene by *Pseudomonas putida* organisms to form catechol.[12] Moreover, a Dewar-dioxetane-like system was suggested to be an intermediate in the oxidation of catechol by non-heme iron-dependent dioxygenases to form muconic acid.[33] In this reaction, both *cis,cis* and *cis,trans* isomers of the muconic acid are observed.[34] Although the dioxetane-like species has been discarded as intermediates based on $^{18}O_2$ labelling studies[35] and theoretical calculations,[36,37] it is still worth analyzing the reactivity of these species because the mechanism is still not clear for both dioxygenase model systems and for the carotenoid oxygenases.[38,39] The argument that lack of light emission excludes a dioxetane mechanism[40] might not be correct because the O-O bond can be either cleaved with the help of an electron donor, or possibly by the involvement of dark photochemistry.

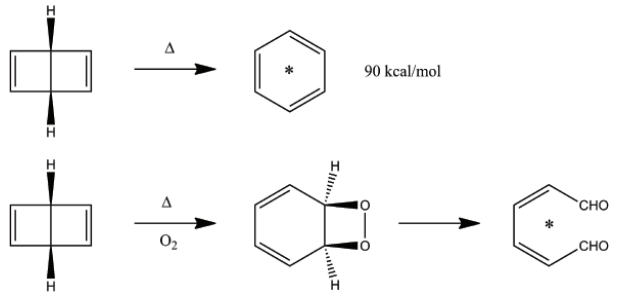

Fig. 3 Suggested thermal reaction paths of Dewar benzene decomposition in (a) absence and (b) presence of molecular oxygen. The last step of model (b) has been studied in the present article.

Thus, the aim of this article is to study the dark photochemistry of 1,3-butadiene through the thermal decomposition of Dewar dioxetane using state-of-the-art quantum chemistry methods and accurate reaction-path computational strategies. On the basis of the findings obtained in previous works on 1,2-dioxetane,[21,41] the target molecule of the present work is expected to have three decomposition channels, thermal and excited-state singlet and triplet dissociations. Regarding the photochemistry of 1,3-butadiene, experiments have reported a complete absence of fluorescence after UV irradiation, which indicates a fast radiationless decay to the ground state.[42–44] This is supported by theoretical studies in which the mechanism is described as follows.[45–48] First, photoexcitation promotes the molecule to the spectroscopic (or bright) state, which accounts for the largest oscillator strength. Second, the molecule relaxes the extra energy evolving through a conical intersection (CI) to a dark singlet excited state. This state lies very close in energy at the Franck-Condon region and it is stabilized along the relaxation coordinate of the initially populated state. Finally, another non-adiabatic process takes place funneling the system to the ground state via a second CI. The whole process is driven by torsion of the C-C bonds, which might give rise to either (a) a non-reactive decay, (b) a photochemical single- or double-bond isomerization, or (c) the formation of cyclobutene or bicyclo[1,1,0]butane. The first step of the dark photochemistry process is obviously different with respect to the photo-induced process because the point at which the system reach the excited state differs in both types of phenomenon. Therefore, an accurate theoretical study of the dark photochemistry requires to begin with the characterization of the thermal dissociation process. In such manner, the reaction coordinate that transfer the reactivity into the photochemical channel of the target molecule is determined. This has been the approach used in the present work.

The study is subsequently structured as follows. The computational details with regards to the electronic structure calculations are considered in the following section. The results are then compiled and described. Next, a discussion on the chemiluminescence and dark photochemistry mechanisms is provided. Finally, the conclusions are stated.

2 Computational Details

Geometry optimizations of the stationary points and minimum energy path (MEP) and intrinsic reaction coordinate (IRC) searches were carried out by employing the complete-active-space self-consistent field (CASSCF) method[49] in conjunction with the atomic natural orbital (ANO-RCC)[50] basis set contracted to O,C[$3s2p1d$]/H[$2s1p$] (hereafter ANO-RCC-VDZP). Additional complete-active-space second-order perturbation theory (CASPT2) energy calculations were performed at the CASSCF optimized geometries improving the basis set from double- to triple-ζ quality, O,C[$4s3p2d1f$]/H[$3s2p1d$] (hereafter ANO-RCC-VTZP).[51] As it was proved in the 1,2-dioxetane study,[21] increasing the size of the basis set to even larger basis sets as well as CASPT2 geometry optimization do not change the qualitative and quantitative description of the chemical process. Therefore, we confined our calculations by employing the CASPT2/ANO-RCC triple-ζ. In the CASPT2 method, accidental near-degeneracies may occur between the wave function and the first-order correction due to weakly interacting intruder states and the perturbation treatment becomes unstable. This is a common situation when applying CASPT2 on medium- to large-size molecular systems. To solve this problem, an imaginary level shift of 0.2 a.u. was used.[52]

The multi-state (MS) approach[53] of the CASPT2 method was also employed throughout to analyze state-interaction effects of the CASPT2 wave functions. In addition, it allows to compare the present findings with those of previous works using the MS-CASPT2 level.[21,22] The MS and state specific (SS) CASPT2 approaches show no significances in the energies and wave functions. This is due to the small off-diagonal elements of the effective Hamiltonian matrix built in the MS computations (lower than 2-3 kcal/mol). In the present work, all the reported energy values correspond to the SS-CASPT2 level (for simplicity, we have used CASPT2 instead of SS-CASPT2 in our tables). Throughout the CASPT2 calculations, core orbitals of non-hydrogen atoms were frozen and the standard ionization potential electron affinity (IPEA) modification of the zeroth-order Hamiltonian with 0.25 value was applied.[54]

On the basis of the previous study with 1,2-dioxetane,[21] a similar two-step biradical mechanism can be expected here for the decomposition of Dewar dioxetane to 2,4-hexadienedial. The biradical mechanism implies that the C_2-C'_2 bond breaking occurs after terminating the O_1-O'_1 rupture (see Fig. 4). In the first step the O_1-O'_1 bond breaking occurs (TS_{S_0}), then the system enters to a biradical region in which four singlet and four triplet states are degenerated. In the next step the C_2-C'_2 rupture comes into action (TS_{S_1,T_1}). Finally, after the C_2-C'_2 cleavage, the system twists around the C_3-C_4-C'_4-C'_3 dihedral angle to produce 2,4-hexadienedial.

Taking into account the features of the described mechanism, a selection for the active space in the CASSCF calculations can be done. The amount of orbitals and electrons which are expected to be the most relevant for the chemiluminescence process of this molecule are 16 and 14, respectively. This corresponds to the C_2-C'_2, O_1-O'_1, C_2-O_1, C'_2-O'_1 σ bonding and σ* antibonding,

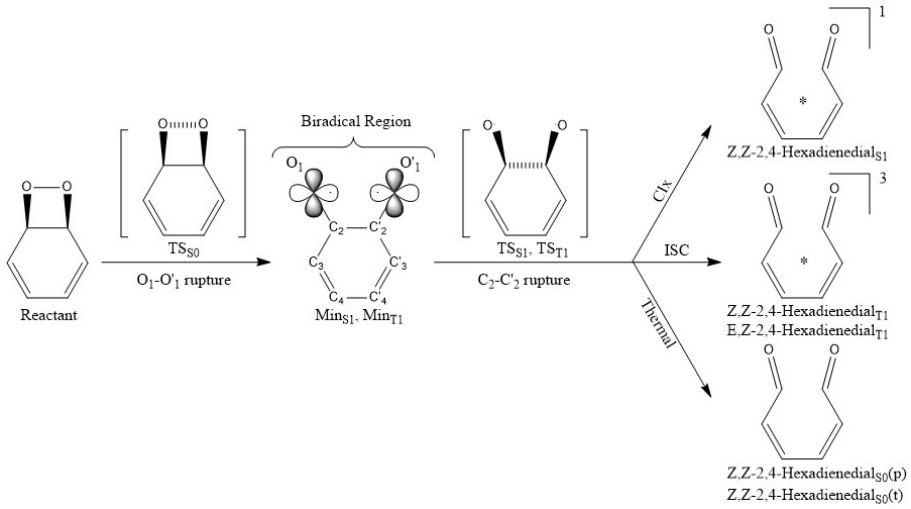

Fig. 4 Decomposition mechanism of Dewar Dioxetane in which the O-O breakage occurs through the first step. Then the system enters to a biradical region in which four singlet and four triplet states are degenerated. After that the C-C rupture comes into action and produces different products. Atom labeling and oxygen lone pair orbitals relevant in the biradical region are shown.

C_3-C_4, C'_3-C'_4 π bonding and π* antibonding orbitals, as well as two oxygen lone-pair orbitals (see Fig. 4). The corresponding CASSCF/CASPT2 computations would be highly CPU- and time-demanding. However, not all of the mentioned orbitals are important throughout the mechanism. Indeed, a reduced active space of 12 electrons distributed in 10 orbitals is already accurate for the study. Within this CAS space, two groups of orbitals (see Figs. 5 and 6) are relevant in distinct parts of the mechanism as described in the following. In the first steps of the mechanism until the TS_{S_1} or TS_{T_1} (see Fig. 4), the C_2-C'_2 bond is still intact. The lowest-lying four singlet and four triplet excited states are mainly described by configuration state functions involving the O_1-O'_1 σ bonding and σ* antibonding orbitals and the two oxygen lone-pair orbitals. Thus, these orbitals are included in the active space (model 1, Fig. 5). The C_2-C'_2 σ bonding and σ* antibonding orbitals become relevant at the TS_{S_1} or TS_{T_1} and they are also added to the CAS. Regarding the C_2-O_1 and C'_2-O'_1 σ bonding and σ* antibonding orbitals, they do not seem important at the first glance. However, a mixing with the previous orbitals occurs and, therefore, they are needed in the CAS. Conversely, in this part of the reaction mechanism, the C_3-C_4 and C'_3-C'_4 π bonding orbitals are doubly occupied and the π* antibonding orbitals are not occupied in the lowest-lying singlet and triplet states. Hence, it is safe to exclude them from the active space. This is due to the fact that the ring remains planar in the first steps of the mechanism and the C_3-C_4 and C'_3-C'_4 bonds do not change. In the last part of the mechanism (see Fig. 4), the C_2-C'_2 cleavage comes into action. Then, the π and π* orbitals related to the C_3-C_4 and C'_3-C'_4 bonds are crucial and must be included in the CAS (model 2, Fig. 6). Conversely, the σ bonding and σ* antibonding orbitals of the C_2-C'_2 and O_1-O'_1 bonds have occupation numbers close to 2 and, consistently, are excluded from the active space. The accuracy of this approach was confirmed by performing two test calculations with a CAS of 16 electrons in 14 orbitals in the reactant structure and at the TS related to the C_2-C'_2 rupture on the S_1 surface (TS_{S_1}).

Different number of roots were considered in the state average (SA) CASSCF procedure for the geometry optimizations to facilitate the convergence and to solve technical problems caused by root flipping in regions having states close in energy. Nevertheless, the final energies reported here correspond to SA-CASSCF computations with four singlet and four triplet states (S_0, S_1, S_2, and S_3 for singlet and T_1, T_2, T_3, and T_4 for triplet).

Zero-point vibrational energy (ZPVE) and Gibbs free energy corrections at 298 K were numerically calculated using the CASSCF/ANO-RCC-VDZP level.

Spin-orbit coupling (SOC) terms between the singlet and triplet states were calculated within the AMFI and CASSI frameworks[55,56] at the CASPT2/ANO-RCC-VTZP wave function over the mentioned four singlet and four triplet states.

The MOLCAS-7.7 quantum-chemistry package was employed for all the calculations.[57]

3 Results

In this section, we will first compile the geometries of the stationary points and the corresponding energies obtained at the CASPT2/ANO-RCC-VTZP//CASSCF/ANO-RCC-VDZP level. After that, the CASPT2//CASSCF reaction paths obtained for the thermal dissociation (on the S_0) and the decomposition on the lowest-lying singlet (S_1) and triplet (T_1) manifolds will be presented in the range from reactants to products.

3.1 Stationary Points

It was shown in the previous study of 1,2-dioxetane that the chemiluminescence reaction occurs via a two-step biradical mechanism, in which, first, an initial O_1-O'_1 bond rupture takes place and, subsequently, the C_2-C'_2 bond is broken.[21] The very same features apply for the decomposition of Dewar dioxetane. Several relevant structures characterize the mechanism between the reactant and products (see Fig. 4): the TS related to the O_1-O'_1 cleav-

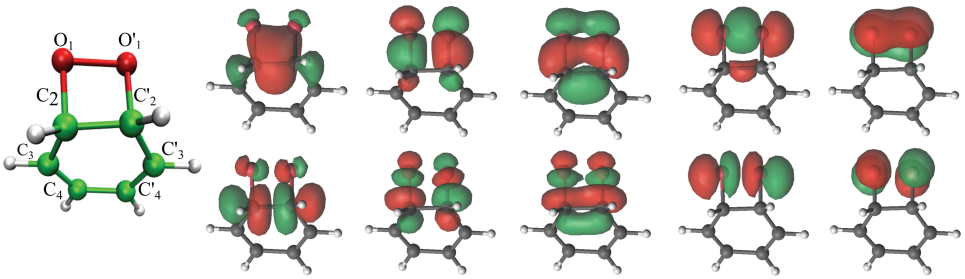

Fig. 5 Natural orbitals relevant in the reactant side and in the first step of the decomposition reaction of Dewar dioxetane related to the dissociation of the O_1-O'_1 (model 1).

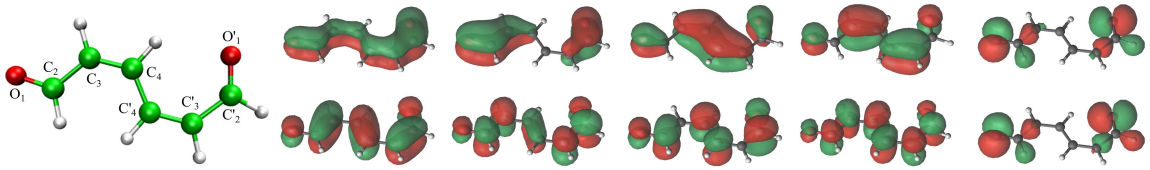

Fig. 6 Natural orbitals relevant in the second step of the decomposition reaction of Dewar dioxetane related to the dissociation of the C_2-C'_2 bond and in the product side (model 2).

age on the singlet ground state manifold ($TS_{S_0,O_1-O'_1}$) in which the four singlet and four triplet excited states become degenerate with S_0, the singlet and triplet biradical minima (Min_{S_1} and Min_{T_1}), the triplet TS related to the C_2-C'_2 bond rupture (TS_{T_1}), and the corresponding TS of C_2-C'_2 cleavage on the singlet excited state (TS_{S_1}). The TS related to the C_2-C'_2 cleavage on the ground-state manifold is quite shallow and therefore difficult to compute. Since the aim of the present study is to comprehend the excited state dissociation (chemiluminescence) of Dewar dioxetane, finding the second TS related to C_2-C'_2 on the ground state has been excluded. Regarding the product of the reaction, the 2,4-hexadienedial is obtained. This molecule has two conjugated C-C double bonds, C_3-C_4 and C'_3-C'_4, which provide the system with Z/E isomerization at each double bond. Additionally, these bonds are weaker and longer in the excited state than in the ground state. Thus, several conformations might be also possible. In particular, six different isomers and conformers of the product in the singlet ($^1C_6H_6O_2$) and triplet ($^3C_6H_6O_2$) states are found as follows (see Fig. 7): (i) the planar *cis-cis* structure, optimized on the singlet ground-state surface [Z,Z-2,4-hexadienedial$_{S_0}$(p)]; (ii) the twisted *cis-cis* structure around the C_4-C'_4 bond, optimized also on the S_0 surface [Z,Z-2,4-hexadienedial$_{S_0}$(t)]; (iii) the *trans-cis* structure, optimized on the S_0 surface (E,Z-2,4-hexadienedial$_{S_0}$); (iv) the *trans-cis* structure, optimized on the surface of the first triplet excited state with $\pi \rightarrow \pi^*$ nature (E,Z-2,4-hexadienedial$_{T_1}$); (v) the *cis-cis* structure, optimized on the surface of the first singlet excited state with $n\pi^*$ nature (Z,Z-2,4-hexadienedial$_{S_1}$); (vi) the *cis-cis* structure, optimized on the T_1 surface with $n\pi^*$ nature (Z,Z-2,4-hexadienedial$_{T_1}$).

Table 1 compiles the most relevant geometrical parameters for

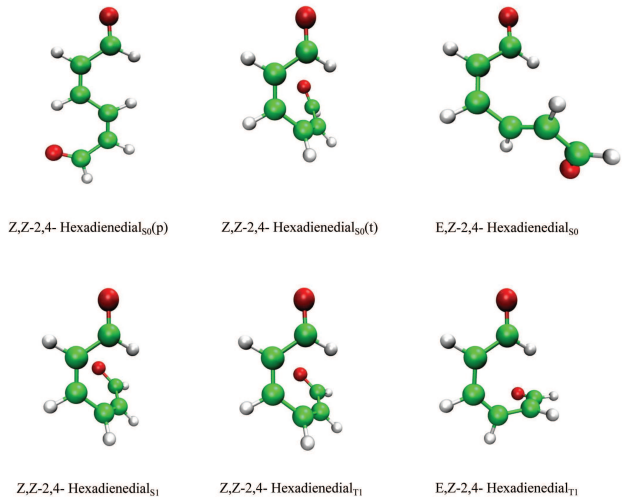

Fig. 7 Optimized product structures of the thermal dissociation of Dewar dioxetane in the ground and the singlet and the triplet lowest-lying excited states. The Z,Z- and E,Z- prefixes refer to *cis,cis-* and *trans,cis-* structures, respectively. Also the (p) and (t) suffixes refer to planar and twisted structures.

the stationary points of the chemiluminescence mechanism of Dewar dioxetane. In comparison to 1,2-dioxetane,[21] the starting geometry (React) has almost the same O_1-O'_1 and C_2-C'_2 bond distance, whereas the O_1-C_2-C'_2-O'_1 dihedral angle is 10.5 degrees instead of the value of 17 degrees for 1,2-dioxetane. The TS_{S_0} has a similar dihedral angle of 33.9 degrees (37 degrees in 1,2-dioxetane). In contrast to 1,2-dioxetane, in which the dihedral angle for the Min_{S_1} and Min_{T_1} and their corresponding TSs ($TS_{S_1(70)}$ and $TS_{T_1(70)}$) was almost 70 degrees, the optimized dihedral angle of the related structures in Dewar dioxetane is 45 degrees, due to conjugation and steric hindrance. For the same reason, the two minima of Min_{S_1} and Min_{T_1} with 180 degrees and their corresponding TSs in 1,2-dioxetane were not found in Dewar dioxetane. Regarding the reaction products, larger differences appear as the result of the presence of the conjugated C-C double bonds and the closed structure. It provides the molecule with a much reacher excited-state chemistry as shall be described in the following sections.

Table 1 Geometrical Parameters of Dewar Dioxetane Optimized at the CASSCF/ANO-RCC-VDZP Level of Theory (Bond lenghts are in Å and dihedral angles are in degree)

	C_2-C'_2	O_1-O'_1	O_1-C_2-C'_2-O'_1
REACT	1.53	1.58	10.46
TS_{S_0}	1.54	2.29	33.95
Min_{S_1}	1.56	2.78	45.5
Min_{T_1}	1.56	2.79	45.03
TS_{T_1}	1.96	2.98	48.33
TS_{S_1}	1.98	3.01	50.89
Z,Z-2,4-Hexadienedial$_{S_0}$ (p)[a,b]	5.44	6.62	0.58
Z,Z-2,4-Hexadienedial$_{S_0}$ (t)[b]	3.63	3.81	27.51
E,Z-2,4-Hexadienedial$_{S_0}$ [a]	4.63	6.41	124.22
E,Z-2,4-Hexadienedial$_{T_1}$ $^3(\pi\pi^*)$	3.76	5.09	82.75
Z,Z-2,4-Hexadienedial$_{S_1}$ $^1(n\pi^*)$	3.49	3.82	51.33
Z,Z-2,4-Hexadienedial$_{T_1}$ $^3(n\pi^*)$	3.53	3.91	51.82

[a] The Z,Z- and E,Z-Hexadienedials refer to the *cis,cis* and *trans,cis* structures, respectively.
[b] The appendices *p* and *t* correspond to the planner and twisted products, respectively.

Table 2 compiles the relative energies of the main stationary points at several CASSCF and CASPT2 levels of increasing accuracy. ZPVE and Gibbs free energy corrections can be found in Table S5 of the Supporting Information. From the comparison of the relative energies, the effects of dynamic electron correlation, MS treatment of the CASPT2, ZPVE and entropy factors can be analyzed. It can be seen that, although the CASSCF method is accurate enough for geometry optimization of Dewar dioxetane, energy values are dramatically affected by the dynamical correlation. This can be clearly seen at, for instance, the TS_{S_0} structure, in which CASSCF underestimates the activation energy by 11.3 kcal/mol due to the lack of dynamical correlation. Nonetheless, as it was shown in 1,2-dioxetane,[21] the CASSCF geometries are accurate enough and the geometry optimization at the CASPT2 level is not required. The ZPVE corrections indicate that each bond dissociation implies a decrease of the activation energy of around 2 kcal/mol. The bond dissociation also causes a change in the entropy of the molecule along the mechanism as well.

The comparison of the energy profile of Dewar dioxetane () with that of 1,2-dioxetane (see Table 2 of the Ref.[21]) shows

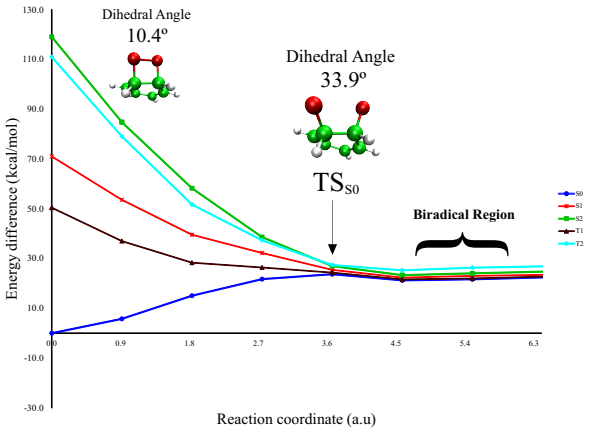

Fig. 8 CASPT2/ANO-RCC-VTZP//CASSCF/ANO-RCC-VTZP IRC computed on the S_0 state from the $TS_{S_0,O_1-O'_1}$. The biradical region in which all the states are degenerated or nearly-degenerated is clearly shown immediately after the TS_{S_0}.

that the same amount of energy is required to reach the TS_{S_0} (25 kcal/mol for both molecules). In contrast, the relative energy between the TS_{T_1} and TS_{S_1} is lower in Dewar dioxetane (3 kcal/mol) than in 1,2-dioxetanes (more than 5 kcal/mol in 1,2-dioxetane). It is worth mentioning here that the general precision of the methodology employed here is around 5 kcal/mol. Therefore, the S_1 excited state is expected to be more easily populated through the thermal decomposition in Dewar dioxetane than in 1,2-dioxetane.

3.2 Ground-state Dissociation

IRC computations at the CASPT2//CASSCF/ANO-RCC-VDZP level from the TS_{S_0} connects the reactant (React) and the biradical region (Min_{S_1}) in which four singlet and four triplet states are degenerate (see Fig. 8). Once the molecule leaves this region of degeneracy, MEP calculations initiated immediately after the Min_{S_1} on the ground state (see Figure S1) clearly show an evolution toward the Z,Z-2,4-hexadienedial$_{S_0}$ (t) structure. This is a twisted geometry of the Z,Z-2,4-hexadienedial$_{S_0}$ (p) species, with a C_3-C_4-C'_3-C'_4 twisting angle of 66.71 degrees (see Fig. 7). The rotation around the mentioned angles shall finally produce the Z,Z-2,4-hexadienedial$_{S_0}$ (p) isomer.

On the basis of the IRC and MEP, the mechanism for the ground-state dissociation can be described. First, the O_1-C_2-C'_2-O'_1 torsion and consequently an O_1-O'_1 bond stretching guide the system from the reactant to the transition state related to the O_1-O'_1 cleavage. Next, when the O_1-O'_1 dissociates, the stretching of the C_2-C'_2 bond comes into action and brings the molecule from the TS_{S_0} structure to the product (2,4-hexadienedial). The activation energy for this mechanism (TS_{S_0}) is 24.1 kcal/mol.

Fig. 8 clearly shows that at the TS_{S_0} all the four singlet and four triplet considered states are degenerated. Moreover, large SOC values are obtained between the singlet and triplet states (see Table S6). Hence, in this region of the reaction path, biradical region, there is a strong non-adiabatic interaction that will split

Table 2 Relative energies at T = 298 K (kcal/mol) of the main stationary structures of thermal decomposition of Dewar benzene at different levels of theory (see text)

	CASSCF/DZ	CASPT2/TZ//CASSCF/DZ	MS-CASPT2/TZ//CASSCF/DZ	ZPVE	Gibbs
REACT	0.0	0.0	0.0	0.0	0.0
TS_{S_0}	13.9	25.2	25.2	23.8	24.1
Min_{S_1}	14.3	22.7	22.7	21.5	21.3
Min_{T_1}	11.2	21.8	21.8	20.3	20.2
TS_{S_1}	33.3	32.1	32.1	27.9	27.4
TS_{T_1}	29.5	29.0	28.9	24.9	24.6
Z,Z-2,4-Hexadienedial$_{S_0}$(p)	-47.9	-70.5	-71.4	-72.5	-74.8
Z,Z-2,4-Hexadienedial$_{S_0}$(t)	-65.6	-62.3	-62.5	-62.2	-66.9
E,Z-2,4-Hexadienedial$_{S_0}$	-68.6	-64.4	-64.6	-67.4	-69.5
E,Z-2,4-Hexadienedial$_{T_1}$ $^3(\pi\pi^*)$	-22.2	-15.2	-15.2	-19.9	-21.9
Z,Z-2,4-Hexadienedial$_{S_1}$ $^1(n\pi^*)$	4.8	7.3	7.2	3.8	2.7
Z,Z-2,4-Hexadienedial$_{T_1}$ $^3(n\pi^*)$	-5.9	5.0	4.7	0.7	-0.9

the population among the states. This part of the reaction has the same energetics as 1,2-dioxetane (see Figure 5 of Ref.[21]).

3.3 Dissociation on the T_1 Manifold

An IRC search on the second TS ($TS_{T_1,C_2-C_2'}$) in the T_1 state connects the minimum on the biradical region (Min_{T_1}) to the E,Z-2,4-hexadienedial$_{T_1}$ structure (see Fig. 9). The first points along the T_1 MEP show that all the states are nearly degenerated until the TS_{T_1} (18.9 a.u). Along these points -biradical region- the nature of the S_1 and T_1 states is $n\pi*$. The same nature characterizes the state at the TS_{T_1} point. Immediately after the TS_{T_1} (22.05 a.u), an adiabatic transformation takes place on the T_1 IRC from $n\pi^*$ to $\pi\pi^*$. Next, the $\pi\pi^*$ nature of the T_1 state remains until the minimum of E,Z-2,4-hexadienedial$_{T_1}$. This transformation can be easily seen following the diabatic representation of the PESs (see dashed lines in Fig. 9). Thus, an energy inversion between the $n\pi^*$ and $\pi\pi^*$ diabatic states takes place. The $n\pi^*$ state becomes higher in energy and the IRC continues with a $\pi\pi^*$ nature. At the end of the IRC, a singlet-triplet crossing (STC) with the S_0 surface is obtained (energy gap of 0.87 kcal/mol). At this region, the system features a twisted C_4-C'$_4$ bond and diradical character, with two unpaired electrons on the C atoms. (The lowest $\pi\pi^*$ triplet states of dienes are explained in details in Ref.[58,59]) In this diradical model, the molecule can decay to the ground state surface in a similar non-adiabatic process as the photoisomerization of ethylene-based systems such as retinal.[60] At the STC crossing point, a large SOC is computed (see supporting information Table S6), which indicates a large probability for population transfer to the ground-state surface. From this crossing, the S_0 MEP clearly shows that the system arrives to the E,Z-hexadienedial$_{S_0}$ structure, which is a higher-energy isomer in comparison to the Z,Z-hexadienedial$_{S_0}$(p,t) species produced in the thermal dissociation (see Fig. 10).

3.4 Dissociation on the S_1 Manifold

The exploration of the S_1 MEP shows that the TS_{S_1} is connected to the biradical region (Min_{S_1}) from the left and to the Z,Z-hexadienedial$_{S_1}$ product structure from the right side (see Fig. 11). The first points after Min_{S_1} along the S_1 PES shows the same behavior as that on the T_1 manifold. The nature of the states in the TS_{S_1} region (18.9 a.u) is $n\pi^*$. In contrast to the triplet, the energy of the singlet $\pi\pi^*$ state at the TS region is much higher. In fact, it is not present among the four roots computed. As a consequence, no change of the nature of states occurs after the TS along the IRC. The MEP finally ends in the excited Z,Z-2,3-hexadienedial$_{S_1}$ species, which is the same isomer as in the thermal ground-state dissociation (see Figs. 7 and 11).

4 Discussion

Here, the findings presented in the previous section are discussed. Firstly, we focus on the thermolysis of Dewar dioxetane, the chemiexcitation process, and the light-emission properties. Secondly, the aspects related to the dark photochemistry of 1,3-butadiene are analyzed in detail.

4.1 Chemiluminescence Mechanism of Dewar Dioxetane

As described in the Introduction, McCapra reported a light emission from the heating of Dewar benzene, although the mechanism giving rise to it was not proved.[31] On the basis of the present CASPT2//CASSCF findings, this experimental study might be interpreted. The chemiluminescence mechanism of Dewar dioxetane occurs as follows. First, an activation energy of 24.1 kcal/mol related to the O_1-O'$_1$ bond breaking is required to reach the biradical intermediate in which an energy degeneracy exists between the lowest-lying four singlet and triplet states of the molecule. In this region the population can be transferred to the singlet excited state. Moreover, it can be transferred to the triplet excited state, taking into account the significant spin-orbit coupling (around 20 cm^{-1}, for details see supporting information Table S6). A second energy barrier, related to the C_2-C'$_2$ bond breaking, is needed to dissociate the molecule in the excited state surface, with a slightly lower activation energy on the triplet manifold. The CASPT2 Gibbs free energies are 24.6 and 27.4 kcal/mol for the triplet and singlet TSs, respectively. Hence, the lowest-energy dissociation mechanism on the excited state corresponds to bond breaking via the triplet surface. This channel gives rise, however, to a radiationless decay via an STC crossing of diradical character. The structure that characterizes the STC point is E,Z-

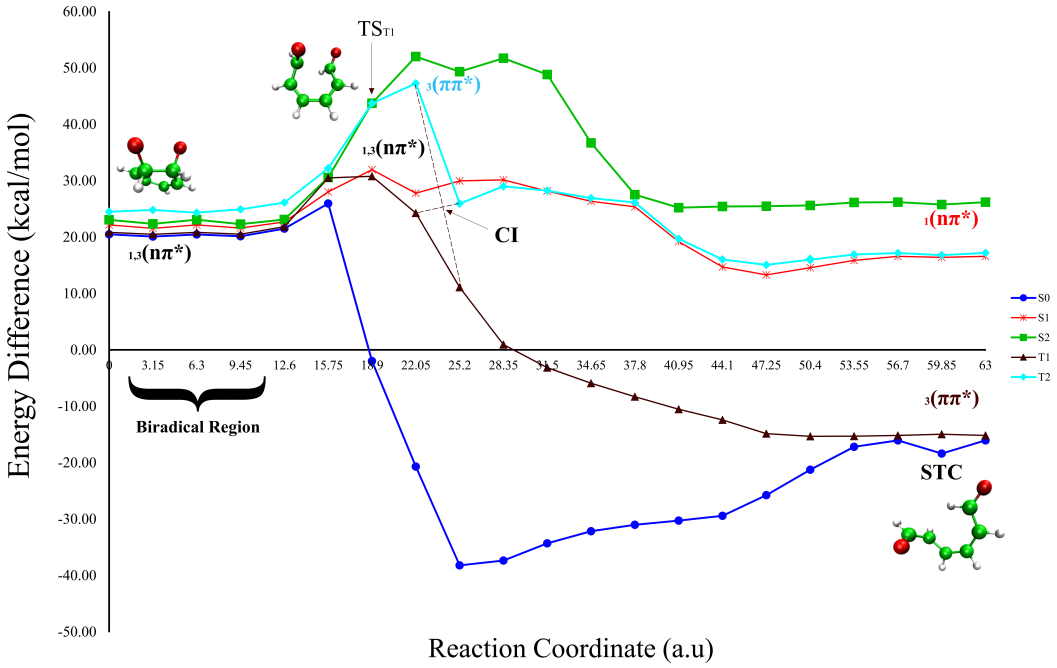

Fig. 9 CASPT2/ANO-RCC-VTZP//CASSCF/ANO-RCC-VDZP IRC computed on the T_1 state from the $TS_{T_1,C_2-C_2'}$. The nature of the ground and lowest-lying singlet and triplet excited states is shown along the IRC. The crossing points (CI and STC) which are relevant for the decomposition mechanism of Dewar dioxetane on the triplet T_1 manifold are indicated. The structure E,Z-2,4-hexadienedial$_{T_1}$ is found at the end of the IRC toward the product.

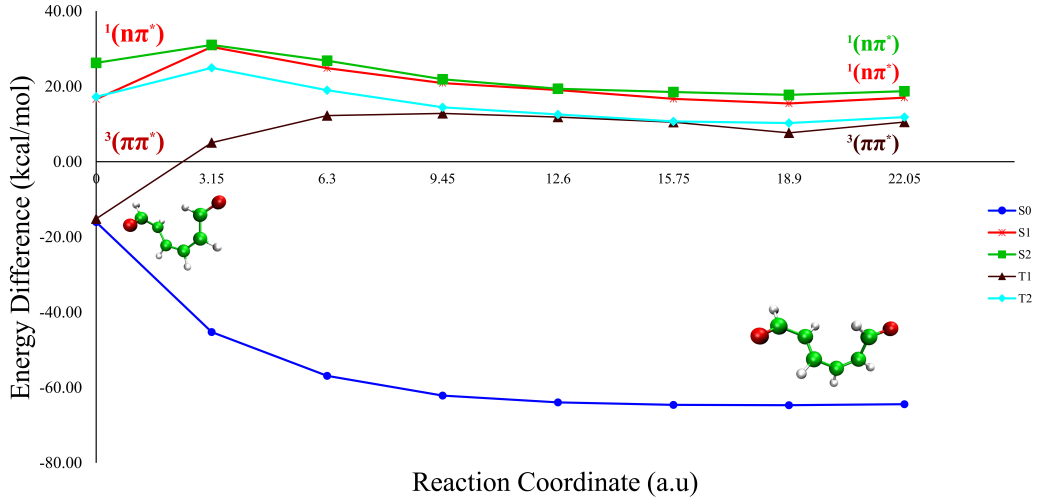

Fig. 10 CASPT2/ANO-RCC-VTZP//CASSCF/ANO-RCC-VDZP MEP computed on the S_0 state from the STC crossing between the T_1 and S_0 states. The product E,Z-2,4-Hexadienedial$_{S_0}$ is found at the end of the MEP.

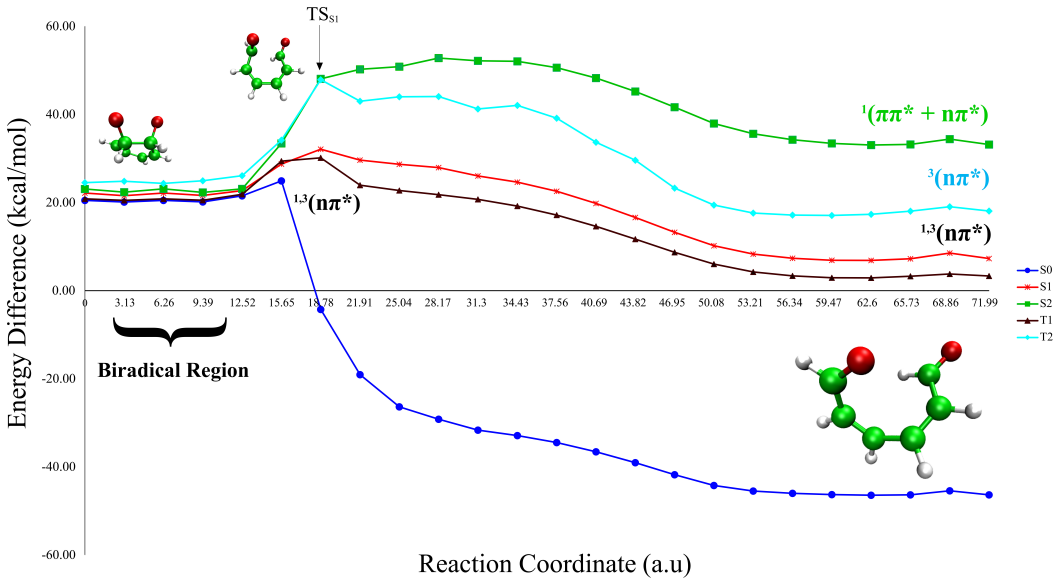

Fig. 11 CASPT2/ANO-RCC-VTZP//CASSCF/ANO-RCC-VDZP IRC computed on the S_1 state from the $TS_{S_0,C_2-C_2'}$. The excited product Z,Z-2,4-Hexadienedial$_{S_1}$ is found at the end of the MEP.

2,4-hexadienedial$_{T_1}$ (see Fig. 7). This non-radiative pathway indicates that light emission should not be considered the outcome of the decomposition of Dewar dioxetane, or related systems, in all the conditions. Similarly, the lack of light emission might not be a valid argument to discard mechanisms based on dioxetane intermediates, as it was done in some studies on enzymatic oxidation by dioxygenases.[40]

Luminescence in the decomposition reaction of Dewar dioxetane would require slightly higher thermal energies. Then, the dissociation mechanism on the singlet excited state would be also activated. According to the IRC computations, the system would evolve on the singlet manifold toward the equilibrium structure, which corresponds to the twisted Z,Z-2,4-hexadienedial$_{S_1}$. The CASPT2//CASSCF value for the vertical emission energy from this point (fluorescence) is 53.6 kcal/mol (532 nm).

In summary, a non-efficient chemiluminescence mechanism is predicted for the decomposition reaction of Dewar dioxetane due to the presence of a radiationless decay on the lowest-energy dissociation channel on the excited triplet states. Moreover, in contrast to 1,2-dioxetane, in which the chemiluminescence process features a triplet emission quantum yield larger than fluorescence, light emission in the decomposition of Dewar dioxetane (only possible at higher temperature) is predicted to be originated from the singlet excited state.

4.2 Dark Photochemistry of 1,3-Butadiene

By means of combining 1,2-dioxetane and 1,3-butadiene and performing the thermal dissociation of the resulting compound, Dewar dioxetane (see Fig. 2), we can access the photochemistry of the polyene (butadiene). It is worth noting, however, that the molecular structure (and the PES region) at which the system reaches the excited state of 1,3-butadiene is different as compared to the geometry that initiates the photo-induced process.[45–48] As described in the Results section, only the dissociation on the triplet manifold brings the reactivity on the photochemical channels of butadiene. The reason for that is the presence of a low-lying triplet $\pi\pi^*$ state which couple with the $n\pi^*$ state at the region of the PESs after the TS related to the dissociation of the C-C' bond (22.05 au in Fig. 9). Conversely, the singlet $\pi\pi^*$ state lies well above the singlet $n\pi^*$ state and do not show a $n\pi^*$ to $\pi\pi^*$ adiabatic transformation. To comprehend this, it is useful to turn to basic molecular orbital (MO) theory. The singlet-triplet energy splitting between states of the same nature (in this case, $n\pi^*$ or $\pi\pi^*$) is proportional to the exchange integral[61]

$K_{12}(n\pi^*) = \langle\psi_n(1)\psi_{\pi^*}(2)|\frac{1}{r_{12}}|\psi_n(2)\psi_{\pi^*}(1)\rangle$, or $K_{12}(\pi\pi^*) = \langle\psi_\pi(1)\psi_{\pi^*}(2)|\frac{1}{r_{12}}|\psi_\pi(2)\psi_{\pi^*}(1)\rangle$,

where ψ_n, ψ_π, and ψ_{π^*} are the orbitals with unpaired electrons in the electronic configurations describing the electronic state and r_{12} is the electron-electron distance. K_{12} is greater than zero and depends on the "penetration" between the orbitals, which is clearly much larger in the $\pi\pi^*$ excited state as compared to the $n\pi^*$ state. Accordingly, the $n\pi^*$ states should appear close in energy, while the $\pi\pi^*$ states should show a much larger energy splitting, being the triplet state at lower energies. This is exactly the behavior found in the present results.

Once the system reaches the triplet $\pi\pi^*$ state, the double bonds of the butadiene moiety become larger and subsequently a radicaloid configuration describes the wavefunction of this state, while one of the double bonds twists and the PES of the triplet state becomes degenerate with that of the ground state. Thus, a STC point is reached which mediates a radiationless decay to the ground state. From the STC branching point, the minimum energy pathway, according to the MEP, implies the evolution to the ground-state E,Z structure. Therefore, a Z,Z to E,Z (*cis,cis* to *trans,cis*) photoisomerization takes place. Note that from the STC there should be another route which will bring the system to the same isomer. *Ab initio* non-adiabatic molecular dynamics, which

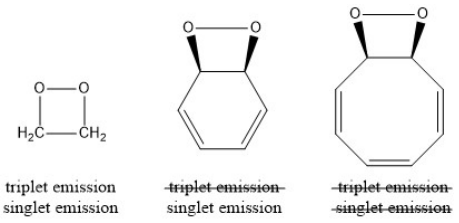

Fig. 12 Estimated trends for the chemiluminescence of 1,2-dioxetane (left) and the molecules formed by 1,2-dioxetane plus 1,3-butadiene (center) and 1,2-dioxetane plus 1,3,5-hexatriene (right), see text.

are out of the escape of the present work, would be helpful for determining the distribution of isomers.[62,63]

The chemiluminescence mechanisms of 1,2-dioxetane and Dewar dioxetane show important differences. Whereas the former is completely driven by the $n\pi^*$ states, the triplet $\pi\pi^*$ state plays a relevant role in the latter. Clearly, the reason is the larger π conjugation of the hexadienedial product as compared to formaldehyde, which decreases the energy of the $\pi\pi^*$ states with respect to that of the $n\pi^*$ states. In the "butadiene+dioxetane" system, this stabilization is not large enough to allow coupling of the singlet states. However, enlarging the polyene moiety, it can be expected that at some point the singlet $\pi\pi^*$ might stabilize enough its energy to allow the interaction with the $n\pi^*$ state, thus opening the photoisomerization channel also on the singlet manifold. In such case, neither triplet nor singlet emission would be expected to be the main decay processes, as illustrated in Fig. 12.

Finally, one might extrapolate the *cis* to *trans* transformation of butadiene to polyenes and flexible π-conjugated systems in general and wonder if this type of processes might be of interest. To answer this question, it is worth reminding that photoisomerizations are relevant in biorganisms: photon-induced isomerizations are the primary event in many processes including vision, ion pumping, and photoaxis.[64,65] Thus, Nature would benefit if the same reactivity could be reached in other manners rather than by irradiation because the photo-induced chemistry would also be possible in the darkness. This view is in agreement with that of some other scientists who postulated in the past that certain peroxidase enzymes make use of dark photochemistry by catalyzing the thermolysis of dioxetane/dioxetanone intermediates.[4,5,12] To date, no evidences have been found proving an intra-molecular sensitized photochemical mechanism in biological systems. This might be in part due to the fact that the experimental detection of the highly reactive chemiluminophore intermediates in the enzymes is a difficult task. Much clear seems to be the relevance of the chemically-induced excited-state processes in technology, as shown by Ermoshkin *et al.*[3] in a study on how to grow "photopolymers" in dark environments.

5 Conclusions

Dewar dioxetane, which combines 1,2-dioxetane and 1,3-butadiene, has been used in the present work with two purposes. The first part is aimed to determine the chemiluminescence mechanism of the molecule. Next, the objective has been to analyze the dark photochemistry of 1,3-butadiene, that is, the excited-state chemistry reached by the system through the decomposition of the dioxetane moiety. High-level CASPT2//CASSCF optimizations of the stationary points and IRC calculations have been performed to determine the reactive path for three succesive processes, the thermal decomposition of the dioxetane moiety, the population transfer to the lowest-lying singlet and triplet excited states, and the photochemical decay of the system once in the excited state. Similar findings to those found for 1,2-dioxetane are obtained for the dissociation mechanism of Dewar dioxetane at the first stage. It occurs as follows. First, the O_1-O'_1 bond is broken by surmounting an energy barrier of 24.1 kcal/mol and the molecule enters to a biradical entropic trap, in which four singlet and four triplet states are degenerated. In this region, the population is distributed among the ground and excited states. Next, the C_2-C'_2 rupture takes place, which open three decomposition channels, on the ground state or on the singlet or triplet excited states. The activation energy related to this bond cleavage on singlet excited manifold is higher than that of the triplet by an amount of 3 kcal/mol. From here on, differences between the chemiluminescence mechanisms of Dewar dioxetane and 1,2-dioxetane arises. Thus, once in the excited state, the evolution on the singlet manifold maintains the $n\pi^*$ character located in the carbonile moieties, as in 1,2-dioxetane. However, an adiabatic transformation from $n\pi^*$ to $\pi\pi^*$ takes place on the triplet manifold, which delocalize the excitation over the whole π conjugated system. This path was not present in the small system. The result is that fluorescence emission is the decay process for the singlet excited molecule, whereas a radiationless energy deactivation through the ethylene-like STC of the 1,3-butadiene moiety is the main decay process on the triplet manifold. Hence, the isomerization of 1,3-butadiene is activated only on the triplet manifold.

The present findings describe the mechanism that might explain the observed light emission in the study of McCapra on the thermal decomposition of Dewar benzene.[31] Thus, decomposition on the singlet excited state manifold produces an excited species that may decay by fluorescence. On the other hand, dissociation channel on the triplet excited state manifold, which requires lower energies, gives rise mainly to a radiationless decay. Due to the presence of this radiationless channel via the triplet state, a much larger quantum yield of singlet emission rather than triplet emission is predicted for the chemiluminescence of Dewar dioxetane. This is in contrast to the behaviour determined theoretically and meassured experimentally for 1,2-dioxetane. Furthermore, the non-radiative decomposition on the triplet manifold shows that photoisomerizations may take place without light. Thus, instead of radiation, a chemiluminophore, such as a dioxetane group, may be used to excite a target molecule and produce photoreactions. This type of reactivity without light ("dark photochemistry") might play a relevant role in biorganisms in the darkness to allow photoreactivity. It has been shown to be interesting for applications in technology.[3]

6 Acknowledgement

PF thanks Uppsala University for support and RL thanks the Swedish Research Council and the eSSENCE e-science project for funding. DRS acknowledge the Spanish MINECO (*Ministe-*

rio de Economía y Competitividad) for funding through Project No. CTQ2014-58624-P and the *Juan de la Cierva* programme, Grant Number JCI-2012-13431. Half of the computations were performed on resources provided by SNIC through Uppsala Multidisciplinary Center for Advanced Computational Science (UPPMAX) under projects SNIC-2013-1-51 and SNIC-2013-1-267 as well as through the Center for Scientific and Technical Computing at Lund University (LUNARC) under project SNIC 2013/1-138. The other half were carried out in the local cluster Quantum Chemistry of the Excited State of Valencia (QCEXVAL) at the *Universitat de València* (Spain) supported by the Spanish MINECO.

References

1 Navizet, I.; Liu, Y.-J.; Ferré, N.; Roca-Sanjuán, D.; Lindh, R. *Comput. Phys. Commun.* **2011**, *12*, 3064–3076.
2 Zimmerman, H. E.; Keck, G. E. *J. Am. Chem. Soc.* **1975**, *97*, 3527–3528.
3 Ermoshkin, A. A.; Neckers, D. C.; Fedorov, A. V. *Macromolecules* **2006**, *39*, 5669–5674.
4 Adam, W.; Cilento, G. *Angew. Chem. Int. Ed. Engl.* **1983**, *22*, 529–542.
5 Cilento, G.; Adam, W. *Photochem. Photobiol.* **1988**, *48*, 361–368.
6 White, E. H.; Wiecko, J.; Roswell, D. F. *J. Am. Chem. Soc.* **1969**, *91*, 5194–5196.
7 Güsten, H.; Ullman, E. F. *J. Chem. Soc. D* **1970**, 28b–29.
8 McCapra, F.; Perring, K.; Hart, R. J.; Hann, R. A. *Tetrahedron Lett.* **1981**, *22*, 5087–5090.
9 Motoyoshiya, J.; Watanabe, K.; Takizawa, A.; Shimizu, H.; Maruyama, T. *Tetrahedron Lett.* **2014**, *55*, 619–622.
10 Adam, W.; Saha-Möller, C. R.; Schönberger, A. *J. Am. Chem. Soc.* **1997**, *119*, 719–723.
11 Iqbal, J.; Husain, A.; Gupta, A. *Chem. Pharm. Bull.* **2006**, *54*, 519–521.
12 Gibson, D. T.; Cardini, G. E.; Maseles, F. C.; Kallio, R. E. *Biochem.* **1970**, *9*, 1631–1635.
13 Lamola, A. A. *Biochem. Biophys. Res. Commun.* **1971**, *43*, 893–898.
14 Adam, W.; Beinhauer, A.; Epe, B.; Fuchs, R.; Griesbeck, A.; Hauer, H.; Mützel, P.; Nassi, L.; Schiffmann, D.; Wild, D. Genotoxic effects of 1,2-dioxetanes. In *Primary Changes and Control Factors in Carcinogenesis*; Friedberg, T.; Oesch, F., Eds.; Deutscher Fachschriften-Verlag: Wiesbaden, 1986, pp. 64–66.
15 Adam, W.; Andler, S.; Nau, W. M.; Saha-Moller, C. R. **1998**, *J. Am. Chem. Soc. 120*, 3549–3559.
16 Knudsen, F. D.; Campa, A.; Stefani, H. A.; Cilento, G. *Proc. Natl. Acad. Sci. USA* **1994**, *91*, 410–412.
17 White, E. H.; Miano, J. D.; Watkins, C. J.; Breaux, E. J. *Angew. Chem. Int. Ed. Engl.* **1974**, *13*, 229–243.
18 Mano, C. M.; Prado, F. M.; Massari, J.; Ronsein, G. E.; Martinez, G. R., Miyamoto, S.; Cadet, J.; Sies, H.; Medeiros, M. H. G.; Bechara, E. J. H.; Di Mascio, P. *Sci. Rep.* **2014**, *4*, 5938.
19 Ciscato, L. F. M. L.; Augusto, F. A.; Weiss, D.; Bartoloni, F. H.; Albrecht, S.; Brandl, H.; Zimmermann, T.; Baader, W. *ARKIVOC* **2012**, *iii*, 391–430.
20 Adam, W.; Baader, W. J. *J. Am. Chem. Soc.* **1985**, *107*, 410–416.
21 Farahani, P.; Roca-Sanjuán, D.; Zapata, F.; Lindh, R. *J. Chem. Theory Comput.* **2013**, *9*, 5404–5411.
22 Liu, F.; Liu, Y.-J.; Vico, L. D.; Lindh, R. *J. Am. Chem. Soc.* **2009**, *131*, 6181–6188.
23 Roca-Sanjuán, D.; Lundberg, M.; Mazziotti, D. A.; Lindh, R. *J. Comput. Chem.* **2012**, *33*, 2124–2126.
24 Yue, L.; Roca-Sanjuán, D.; Lindh, R.; Ferré, N.; Liu, Y.-J. *J. Chem. Theory Comput.* **2012**, *8*, 4359–4363.
25 Liu, F.; Liu, Y.-J.; Vico, L. D.; Lindh, R. *Chem. Phys. Lett.* **2009**, *484*, 69–75.
26 Roca-Sanjuán, D.; Delcey, M. G.; Navizet, I.; Ferré, N.; Liu, Y.-J.; Lindh, R. *J. Chem. Theory Comput.* **2011**, *7*, 4060–4069.
27 Chung, L. W.; Hayashi, S.; Lundberg, M.; Nakatsu, T.; Kato, H.; Morokuma, K. *J. Am. Chem. Soc.* **2008**, *130*, 12880–12881.
28 Navizet, I.; Roca-Sanjuán, D.; Yue, L.; Liu, Y.-J.; Ferré, N.; Lindh, R. *Photochem. Photobiol.* **2013**, *89*, 319–325.
29 Chen, S.-F.; Navizet, I.; Roca-Sanjuán, D.; Lindh, R.; Liu, Y.-J.; Ferré, N. *J. Chem. Theory Comput.* **2012**, *8*, 2796–2807.
30 Chen, S.-F.; Ferré, N.; Liu, Y.-J. *Chem. Eur. J.* **2013**, *19*, 8466–8472.
31 McCapra, F. *Pure Appl. Chem.* **1970**, *24*, 611–629.
32 Criegee, R.; Noll, K. *Eur. J. Org. Chem.* **1959**, *627*, 1–14.
33 Hayaishi, O.; Katagiri, M.; Rothberg, S. *J. Am. Chem. Soc.* **1955**, *77*, 5450.
34 Jastrzebski, R.; van den Berg, D. J.; Weckhuysen, B. M.; Bruijnincx, P. C. A. *Catal. Sci. Technol.* **2015**, *DOI: 10.1039/C4CY01562B*.
35 Mayer, R. J.; Que, L. *J. Biol. Chem.* **1984**, *259*, 13056.
36 Borowski, T.; Siegbahn, Per E. M. *J. Am. Chem. Soc.* **2006**, *128*, 12941–12953.
37 Jastrzebski, R.; Quesne, M. G.; Weckhuysen, B. M.; de Visser, S. P.; Bruijnincx, P. C. A. *Chem. Eur. J.* **2014**, *20*, 15686–15691.
38 Pap, J. S.; Kaizer, J.; Speier, G. *Coord. Chem. Rev.* **2014**, *254*, 781–793.
39 Borowski, T.; Blomberg, M. R. A.; Siegbahn, Per E. M. *Chem. Eur. J.* **2008**, *14*, 2264–2276.
40 Bugg, T. D. H.; Lin, G. *Chem. Comm.* **2001**, *11*, 941–952.
41 Vico, L. D.; Liu, Y.-J.; Krogh, J. W.; Lindh, R. *J. Phys. Chem. A* **2007**, *111*, 8013–8019.
42 Gavin, R. M. J.; Risemberg, S.; Rice, S. A. *J. Chem. Phys.* **1973**, *58*, 3160.
43 Zerbetto, F.; Zgierski, M. Z. *J. Chem. Phys.* **1990**, *93*, 1235.
44 Fuβ, W.; Schmid, W. E.; Trushin, S. A. *Chem. Phys. Lett.* **2001**, *342*, 91–98.
45 Olivucci, M.; Ragazos, I. N.; Bernardi, F.; Robb, M. A. *J. Am. Chem. Soc.* **1993**, *115*, 3710–3721.
46 Celani, P.; Bernardi, F.; Olivucci, M.; Robb, M. A. *J. Chem.*

Phys. **1995**, *102*, 5733.
47 Ruiz, D. S.; Cembran, A.; Garavelli, M.; Olivucci, M.; Fuss, W. *Photochem. Photobiol.* **2002**, *76*, 622–633.
48 Levine, B. G.; Martínez, T. J. *J. Phys. Chem. A* **2009**, *113*, 12815–12824.
49 Roos, B. O. *Advances in Chemical Physics: Ab Initio Methods in Quantum Chemistry Part 2.*; John WILEY and Sons: New York, 1987; pp 399–446.
50 Roos, B. O.; Lindh, R.; Malmqvist, P.-Å.; Veryazov, V.; Widmark, P.-O. *J. Phys. Chem. A* **2010**, *31*, 224.
51 Roca-Sanjuán, D.; Aquilante, F.; Lindh, R. *WIREs Comput. Mol. Sci.* **2012**, *2*, 585–603.
52 Forsberg, N.; Malmqvist, P.-Å. *Chem. Phys. Lett.* **1997**, *274*, 196–204.
53 Finley, J.; Malmqvist, P.-Å.; Roos, B. O.; Serrano-Andrés, L. *Chem. Phys. Lett.* **1998**, *288*, 299–306.
54 Ghigo, G.; Roos, B. O.; Malmqvist, P. *Chem. Phys. Lett.* **2004**, *396*, 142–149.
55 Rubio-Pons, O.; Serrano-Andreés, L.; Merchán, M. *J. Phys. Chem. A* **2001**, *105*, 9664–9673.
56 Strickler, S. J.; Berg, R. A. *J. Chem. Phys.* **1962**, *37*, 814–822.
57 Aquilante, F.; Vico, L. D.; Ferré, N.; Ghigo, G.; Malmqvist, P.-Å.; Neogrády, P.; Pedersen, T. B.; Pitoňák, M.; Reiher, M.; Roos, B. O.; Serrano-Andrés, L.; Urban, M.; Veryazov, V.; Lindh, R. *J. Comput. Chem.* **2010**, *31*, 224.
58 Salem, L. *Pure. Appl. Chem.* **1973**, *33*, 317–328.
59 Salem, L.; Rowland, C. *Angew. Chem. Int. Ed. Engl.* **1972**, *11*, 92–111.
60 González, R.; Olaso-González, G.; Merchán, M.; Coto, P. B.; Serrano-Andrés, L.; Gavarelli, M. *Int. J. Quantum Chem.* **2011**, *111*, 3431–3437.
61 Szabo, A.; Ostlund, N. S. *Modern Quantum Chemistry*; Dover Publications: Inc., Mineola, New York, 1996; p 86.
62 González, L.; Escudero, D.; Serrano-Andrés, L. *ChemPhysChem* **2012**, *13*, 28–51.
63 Mai, S.; Marquetand, P.; González, L.; *Int. J. Quantum Chem.* **2015**, DOI: 10.1002/qua.24891.
64 Dugave, C.; Demange, L. *Chem. Rev.* **2003**, *103*, 2475–2532.
65 van der Horst, M.; Hellingwerf, K. *Acc. Chem. Res.* **2004**, *37*, 13–20.